Crystallization kinetics of mixed amorphous-crystalline nanosystems

A. Mattoni* and L. Colombo†

SLACS-INFM/CNR, Sardinian Laboratory for Computational Materials Science and Dipartimento di Fisica, Università di Cagliari, Cittadella Universitaria, I-09042 Monserrato (Ca), Italy

(Received 23 April 2008; revised manuscript received 20 June 2008; published 8 August 2008)

We investigate at the atomic scale the crystallization of a two-phase amorphous-crystalline system. We focus on the case of textured nanocrystalline silicon here described as a distribution of cylindrical grains embedded into an amorphous matrix. The atomistic results are used to infer a continuum model of the crystallinity evolution and to work out a comparison with Kolmogorov-Johnson-Mehl-Avrami (KJMA) model. At low crystallinity, the phase transformation is dominated by the isolated grain evolution (faceted limited growth). Conversely, at later stages we observe deviations from the KJMA that are mainly due to atomic-scale features. We prove that such effects can be included by using an improved phenomenological version of the KJMA theory.

DOI: 10.1103/PhysRevB.78.075408 PACS number(s): 61.46.Hk

I. INTRODUCTION

Mixed-phase amorphous-crystalline (*a-c*) systems are both of technological and theoretical relevance.[1] In particular, this is the case of nanocrystalline (NC) materials,[2] where a distribution of nanosized crystal grains is embedded into an amorphous matrix. NC systems are useful for advanced optoelectronics,[3] structural engineering,[4–6] and many other technological applications.[2] Remarkably, NC-silicon films[3] are promising systems for low cost photovoltaics since, by controlling the dimension of their grains, it is possible to optimize the absorption coefficient and to improve the photoconversion efficiency. As for structural applications, we mention the case of nanodiamond carbon,[6] which consists of diamond grains dispersed into an otherwise amorphous carbon film. Such systems are used as ultrahard coatings since the nanosized diamonds are able to largely modify the mechanical response, increasing the fracture toughness of the material (particle reinforcing).[5]

NC systems are in most cases thermodynamically metastable. Since the free energy is larger in the amorphous phase than in the corresponding crystalline one (as occurs, for example, for silicon and carbon), *a-c* systems tend to crystallize.[7] It is possible to take advantage of this property in order to synthesize new materials by solid phase crystallization;[1] by high-temperature annealing of an amorphous matrix it is observed the nucleation of crystal seeds and their further growth.[1,7–10] On the other hand, the same metastability may induce an uncontrolled microstructure evolution that can, in turn, deteriorate the properties of the system. Therefore, a comprehensive physical understanding and theoretical modeling of the microstructure evolution of *a-c* biphasic systems is mostly needed and useful for technological impact.

The phase transformation kinetics of *a-c* materials is traditionally described by the well celebrated Kolmogorov-Johnson-Mehl-Avrami (KJMA) theory.[11–14] A first-order phase transformation (e.g., the crystallization from the amorphous phase) is described in terms of two phenomena, namely, (i) the random nucleation of new stable grains within the metastable amorphous phase and (ii) the growth of the nucleated grains. In particular, the KJMA theory provides the fraction of transformed material as a function of time (see Sec. IV). Both the nucleation and growth phenomena are controlled by atomic-scale events. In order to include them into the mesoscopic KJMA theory, two effective laws are required:[15] the time evolution $\nu(t)$ of the isolated grain volume and the number of new grains nucleating during a unit of time, i.e., the nucleation rate $J(t)$. Both functions $\nu(t)$ and $J(t)$ depend on the actual thermodynamic conditions and on the microscopic morphological details of the metastable phase (e.g., the presence of defects and inhomogeneities or local strain), as well as on the growth mechanisms. In general, they are unknown *a priori*. It is customary to describe $\nu(t)$ and $J(t)$ in terms of adjustable parameters that are typically fitted on the experimental data.[16] This procedure is very successful in describing the kinetics of first-order phase transformations. Nevertheless, deviations are sometimes observed like in metals[17] or in silicon.[1] The validity of the KJMA theory has been extensively discussed in the literature.[15,18] As a matter of fact, the KJMA formulation is strictly valid when the following three conditions are fulfilled:[15,18] (i) the nucleation of new crystalline grains occurs everywhere with the same probability (random and uniform nucleation); (ii) the growth of each grain is isotropic and it is not affected by the presence of neighboring grains (isolated growth); and (iii) the volume of an arbitrary grain is much smaller than the total volume of the system.[19]

In many cases of interest the fulfillment of these conditions is questionable[17,20–23] and, therefore, the KJMA theory has been critically readdressed, as briefly outlined in the following.[17,18] Most investigations have focused on the deviations from condition (i), considering, e.g., a position-dependent nucleation.[22] By using lattice Monte Carlo simulations, it has been possible to investigate several nonuniform nucleation phenomena occurring when microscopic inhomogeneities are present,[20] when the nucleation rate is modified in the regions around the growing grains,[22] or, finally, when the nucleation depends on the untransformed fraction (e.g., during soft impingement of grains due to diffusion controlled growth[23]). On the other hand, deviations from the independent and isotropic grain growth [condition (ii)] are expected to be important in covalently (i.e.,

anisotropic) bonded materials. It has been proved that the KJMA theory is still valid when the growth is nonisotropic, provided that the grains are parallel.[18,22] Nevertheless, the validity of the KJMA theory in covalent systems is still a matter of discussion. Alternative kinetic models have been preferred to study crystallization in silicon.[1]

The main difficulty in proving the ability of the KJMA theory to reproduce the experimental data is that, in most cases, the nucleation and growth occur at the same time, so that the two phenomena are entangled.[16] Interesting enough, this is not the case of the site-saturated crystallization.[16] Here the nucleation does not occur but for a very short-time transient (hereafter referred to as the nucleation time t_N) during which all the grains nucleate in the amorphous phase. At $t > t_N$, the crystallization is fully controlled by the grain growth only. Accordingly, the site-saturated regime is particularly favorable to verify the reliability of the KJMA theory to describe crystallization driven by a realistic model of grain growth.

Whatever modification is applied to the KJMA theory to improve its validity, the truly atomic-scale description of the underlying physical phenomena (nucleation and growth) remains out of reach of this continuum model. In order to bypass this conceptual limitation, we performed a molecular-dynamics (MD) investigation on the crystallization of a silicon amorphous system under the condition of site saturation (i.e., in absence of nucleation). Atomistic simulations have already been successfully applied to study the kinetics of growth of an isolated cylindrical grain embedded into amorphous silicon.[7] The present work is aimed at extending our previous investigations to the case of a distribution of grains. After a detailed description of the growth of an isolated grain (Sec. III), we consider the case of an amorphous sample containing a finite number of grains (see Sec. IV). By simulating at the atomic scale the crystallization, we are able to naturally include effects which are not covered by the constitutive hypothesis of KJMA theory (such as the anisotropic growth of silicon grains[7] and their mutual interaction). The atomistic results (discrete in nature) are coarse grained into a mesoscopic model (in the spirit of a phase field model) so as to calculate the deviations from the ideal KJMA theory (Sec. IV) in the realistic crystallization process.

II. LARGE SCALE ATOMISTIC SIMULATIONS OF THE CRYSTALLIZATION KINETICS

We performed constant-temperature constant-volume simulations on a periodically repeated simulation cell, containing an isolated or a distribution of c-Si grain(s) embedded into a-Si. The orthogonal cell has dimensions $L_x = 2.5$ nm, $L_y = 25$ nm, and $L_z = 25$ nm (along x, y, z directions, respectively).

The atomic forces were calculated according to the environment dependent interatomic potential (EDIP),[24] recently applied to study a-c systems.[25] The simulation cell contains $\sim 10^5$ atoms. The temperature of the system was kept fixed by a rescaling velocity thermostat.

The microstructure evolution of the biphasic system (see Fig. 1) was characterized by the average structure factor (SF)

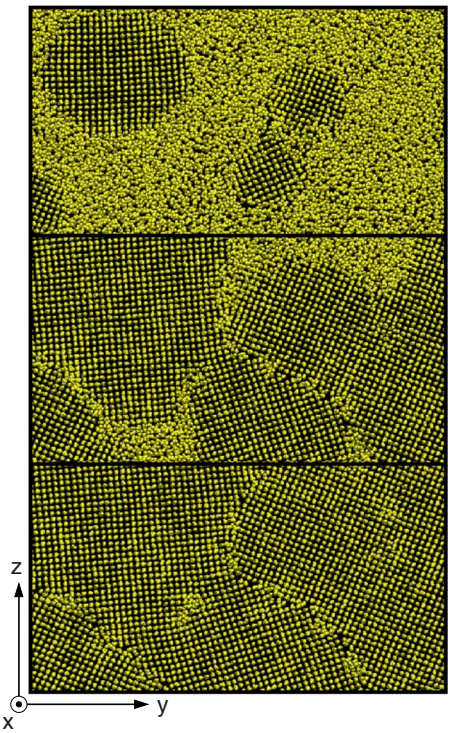

FIG. 1. (Color online) Snapshots of the NC-Si/a-Si crystallization process at 1200 K (y-z planar projection) after 0.5 ns (top), 1.5 ns (middle), and 2.0 ns (bottom).

$\Theta(k)$,[26,27] the k vector $[\frac{a_0}{4}, 0, 0]$ corresponding to the interplanar distance of c-Si along the x direction. The average SF was calculated by first dividing the system into subcells, then by calculating the local structure factor within each subcell, and, finally, by taking the average over all the subcells. Each box was chosen to contain at least several hundreds of atoms. The average structure factor represents an average between the crystalline (Θ_c) and the amorphous (Θ_a) values, weighted by their relative abundance (χ_c and χ_a, respectively),

$$\Theta(T,t) = \chi(T,t)\Theta_c(T) + [1 - \chi(T,t)]\Theta_a(T). \quad (1)$$

In Eq. (1), we set $\chi_a = 1 - \chi(T,t)$ since for the two-phase a-c system we expect $\chi_a + \chi_c = 1$. The crystallinity fraction is straightforwardly computed by Eq. (1),

$$\chi(T,t) = [\Theta(T,t) - \Theta_a][\Theta_c(T) - \Theta_a]^{-1}. \quad (2)$$

It is important to note that the structure factor $\Theta_c(T)$ is a decreasing function of the temperature (as a result of the lattice disorder induced by thermal fluctuations). The fit of present MD data provides a linear dependence of the crystallinity upon temperature

$$\Theta_c(T) = 1 - 1.71 \times 10^{-4} T \quad (3)$$

for any $T < T_{mc}$. T_{mc} is the EDIP melting temperature of c-Si (see Appendix). On the other hand, we found a constant $\Theta_a(T) \sim 0.1$ for any value of T.

In order to validate the above theoretical framework, the crystallinity $\chi(T,t)$ was also calculated by a topological analysis of the bond ring statistics (RS).[28] We assumed that

two atoms are connected if their relative distance is smaller than 2.5 Å. Accordingly, in the perfect diamond structure (at zero temperature) only six-member rings are found and, moreover, on each lattice site 12 different rings merge. Therefore an atom is attributed to the crystalline phase if the number of six-member rings there merging is exactly 12. At finite temperature, as a result of the thermal vibrations, the number of six-member rings merging on an atomic site decreases and rings of different sizes form with a probability distribution that depends on temperature. We attributed an atom of a biphasic system to the crystalline phase if the number of rings is compatible with the same distribution of rings in a monocrystalline sample at the corresponding temperature. Roughly speaking, in the range $1000\ \mathrm{K} < T < 1200\ \mathrm{K}$, an atom is crystalline when the number of six-member rings is greater than eight. Such a choice was validated by an analysis of the atomic positions. It is proved that both criteria (based, respectively, on the notion of structure factor and on ring statistics) provide very similar estimations of $\chi(t,T)$.

The atomistic models of nanocrystalline silicon were obtained by inserting a fixed number N of cylindrical grains (fibers) into the amorphous slab. The fibers were cut away from a perfect silicon crystal in such a way that their [100] crystallographic direction is parallel and aligned along the x direction of the simulation cell (see Fig. 1). Each fiber was then randomly rotated around x to mimic the casual nucleation of grains. We considered two cases: $N=1$ and $N=20$. In the first case, the radius ρ_0 of the grain was chosen equal to 0.3 nm. In the case of a distribution of grains, the radii ρ_0^i $(i=1,\ldots,N)$ were chosen according to the following procedure: (i) N points are selected at random within a y-z plane of the simulation cell; (ii) the minimum distance $d_{\min}$ between points is calculated; and (iii) the radii are generated at random within the range $[\rho_{\min},\rho_{\max}=d_{\min}/2\times 0.4]$. $\rho_{\min}$ was chosen to be larger than the capillarity threshold R^*, namely, the minimum radius for which an embedded grain is thermodynamically stable during a thermal annealing. According to the classical nucleation growth theory (see Sec. III), the free energy of a crystal grain with radius smaller than R^* is dominated by the surface contribution. Therefore, during a thermal annealing it is expected to shrink and to melt into the amorphous phase. Since R^* depends on the actual temperature, we used the largest value in the range of temperature considered. It will be shown in Sec. III that $0.2\ \mathrm{nm} < R^* < 0.5\ \mathrm{nm}$ so that we set $\rho_{\min}=0.5$ nm. By following the above procedure the initial grains have different sizes (and orientations) and they do not touch each other. Furthermore, since $\rho_0^i > \rho_{\min} > R^*$, they are stable and they grow during the applied thermal annealing. This corresponds to the site-saturated crystallization condition.

The systems generated according to the above protocol were equilibrated by ~ 0.3 ns at the temperature of interest. During this time the grains transform from the ideal cylindrical shape to a different morphology that is thermodynamically favorite. The radii of the grains just after the thermalization are referred to as R_0^i, $i=1,\ldots,N$. They depend on temperature $R_0^i=R_0^i(T)\neq\rho_0^i$, $i=1,\ldots,N$. In the case $N=1$ the radius is referred to as $R_0(T)$. The crystallization phenomena were studied during further annealing. In the case of the isolated grain, the effective radius was calculated from the crystallinity χ through the relation $R=(\frac{A_{yz}}{\pi}\chi)^{1/2}$, where $A_{yz}=L_yL_z$ is the lateral area of the simulation cell.

III. ISOLATED GRAIN GROWTH KINETICS

Without nucleation, the crystallization of mixed amorphous-crystalline systems is the result of the grain growth or, that is the same, of the a-c boundary mobility. This occurs since the free energy of the amorphous phase is larger than the crystalline one. If we name g_a and g_c the free energy per unit volume of the amorphous and crystalline phases, respectively, we get $g_{ac}=g_a-g_c>0$. It is possible to define a thermodynamic pressure p acting on an a-c boundary of area S as

$$p=-\frac{dG}{dV}, \tag{4}$$

where dG is the free-energy change associated to an infinitesimal displacement dR of the a-c boundary and $dV=SdR$ is the transformed volume (if $p>0$ the free energy decreases). The work dG necessary to crystallize a volume dV is

$$dG=-g_{ac}dV+\gamma_{ac}dS, \tag{5}$$

where dS is the corresponding variation of the a-c area and γ_{ac} is the interface energy per unit of a-c area. According to Eq. (5), we get

$$p=g_{ac}-\gamma_{ac}\frac{dS}{dV}. \tag{6}$$

In the case of a planar boundary, $dS/dV=0$ and $p=g_{ac}$. In the case of an isolated cylindrical $(D=2)$ or spherical $(D=3)$ grain the surface-to-volume ratio $dS/dV=(D-1)/R$ depends on the radius R. In the cylindrical case the pressure is therefore given by

$$p(R)=g_{ac}\left(1-\frac{R^*}{R}\right). \tag{7}$$

At the capillarity threshold, we get $R^*=(D-1)\gamma_{ac}/g_{ac}$ and $p(R^*)=0$. R^* is easily computed in the case of silicon: since[1] $\gamma_{ac}=(0.1-0.3)\ \mathrm{eV}/S_{\mathrm{at}}$ and $g_{ac}\sim 0.1\ \mathrm{eV}/V_{\mathrm{at}}$, where S_{at} is the a-c area per atom, we obtain $R^*=(1-3)V_{\mathrm{at}}/S_{\mathrm{at}}=0.1-0.4$ nm, where $V_{\mathrm{at}}/S_{\mathrm{at}}=a_0/4$ and a_0 being the c-Si lattice parameter.

The simplest kinetic model for crystallization is the interface limited growth (ILG) model, describing the crystallization process as a sequence of uncorrelated transformations (occurring at the interface) from amorphouslike atoms to crystal-like ones. Each event requires the bypass of a given energy barrier E_b. Accordingly, the interface velocity v turns out to be a function of the pressure p,

$$v=M\alpha^{-1}(1-e^{-p\alpha}), \tag{8}$$

where $\alpha=V_{\mathrm{at}}/(k_BT)$, V_{at} is the atomic volume, and k_B is the Boltzmann constant. $M=\mu e^{-E_b/k_BT}/(k_BT)$ is the a-c mobility and μ is a prefactor related to the material. The exponential dependence of M upon the temperature has been experimen-

tally verified only in the case of planar *a-c* interfaces.[29] Notably, at high temperature $p<1/\alpha$ and the velocity is simply proportional to the pressure,

$$v = Mp. \tag{9}$$

Under this condition $R(t)$ is obtained by solving

$$\frac{dR}{dt} = Mg_{ac}\left(1 - \frac{R^*}{R}\right). \tag{10}$$

The relation between the radius and time is $t = (Mg_{ac}/R^*)^{-1}\{\frac{R}{R^*} - \frac{R_0}{R^*} + \ln[(\frac{R}{R^*}-1)/(\frac{R_0}{R^*}-1)]\}$ providing linear growth $R \sim R_0 + Mg_{ac}t$ at large radii. In fact, for $R > R^*$ Eq. (10) is approximated by a constant velocity,

$$v(R) \sim Mg_{ac}. \tag{11}$$

By studying cylindrical *a-c* boundaries in silicon,[7] we have recently proved that deviations from the ILG model are possible. Such deviations are observed when the microscopic crystallization events are correlated. This is the case of faceted grain growth that we proposed[7] to describe by a power-law growth (PLG) model. Here the mobility M is replaced by an effective radius-dependent *a-c* mobility $M(\frac{\lambda}{R})^{1/q-1}$ and q is an exponent possibly depending on temperature. The corresponding velocity is calculated to be

$$v(R) \sim M\left(\frac{\lambda}{R}\right)^{1/q-1} g_{ac}\left(1 - \frac{R^*}{R}\right). \tag{12}$$

When $R \gg R^*$ we get

$$v(R) \sim Mg_{ac}\left(\frac{\lambda}{R}\right)^{1/q-1} \tag{13}$$

and

$$\frac{dR}{dt} = Mg_{ac}\left(\frac{\lambda}{R}\right)^{1/q-1}. \tag{14}$$

By separating the variables r and t,

$$R^{1/q-1}dR = Mg_{ac}\lambda^{1/q-1}dt, \tag{15}$$

and by integrating over the time interval $[0,t]$ (during which the radius grows from R_0 up to R) we finally obtain

$$R(t) = R_0\left[\Gamma\left(\frac{\lambda}{R_0}\right)^{1/q} t + 1\right]^q, \tag{16}$$

where $\Gamma = \frac{Mg_{ac}}{q\lambda}$. In the limit of a very small crystal seeds (i.e., for $R_0 \to 0$) the previous equation reduces to

$$R(t) = \alpha t^q, \tag{17}$$

where $\alpha = \Gamma^q\lambda$. The grain volume $v(t) = \pi L_x R(t)^2$ is

$$v(t) = \beta t^p, \tag{18}$$

where $\beta = \pi L_x \alpha^2$ and $p = 2q$ for the actual cylindrical case. By using Eq. (16) it was possible to fit the atomistic data. For each given temperature we used the set $\{q, \Gamma, R_0, \lambda\}$ as adjustable parameters and we found that they are temperature dependent.[7] A detailed calculation of this is reported in Appendix. Here we discuss the variation of q upon temperature

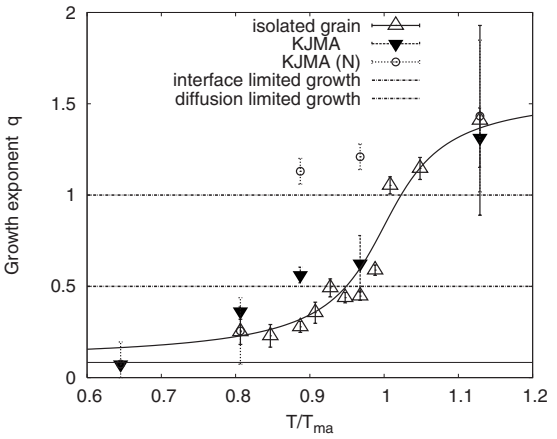

FIG. 2. Growth exponents as a function of temperature calculated in the case of isolated grains (open triangles), distribution of grains according to KJMA (filled triangles), and KJMA-N model (circles).

(see Fig. 2). The exponent $q=0.5$ (corresponding to the case of diffusion-limited growth[7]) is observed in the range of temperatures $0.9 < T/T_{ma} < 1$, just below the EDIP melting temperature T_{ma} of *a*-Si (see Appendix). At lower temperatures the growth exponent is smaller but still positive. Exponents smaller (larger) than 1 correspond to decelerated (accelerated) growth[7] while the case $q=1$ corresponds to the uniform growth. A transition from a decelerated regime to a quasiuniform one is observed at T_{ma}; we attribute such a change to the transition of the amorphous network into a liquid, as predicted by the EDIP model and in agreement with experimental observation.[30] This transition is demonstrated by the observed morphology of the grain boundary changing from a faceted interface (at low temperature) to a smooth cylindrical one (at temperatures higher than T_{ma}).

The result of the fit of Eq. (16) on the atomistic data is reported in Fig. 3. The calculated function $R(t,T)$ completely characterizes the grain growth. For example, the velocity is easily obtained by calculating the derivative with respect to the annealing time $v(t,T) = \frac{dR}{dt}(t,T)$. The plot of the normal-

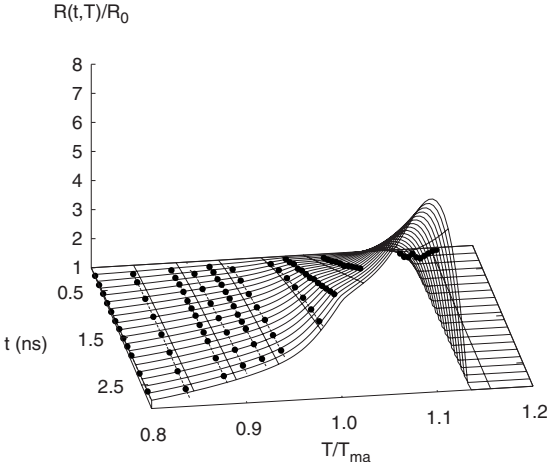

FIG. 3. Grain radius as a function of time and temperature. Symbols represent atomistic data.

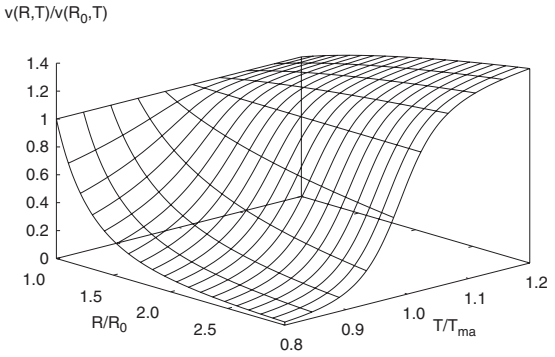

FIG. 4. Grain growth velocity as a function of the grain radius and temperature.

ized $v(R,T)/v(R_0,T)$ velocity is reported in Fig. 4. The curve clearly shows that the growth is decelerated up to $T \sim T_{ma}$, while for $T > T_{ma}$ the growth is uniform or accelerated.

IV. DISTRIBUTION OF GRAINS AND KOLMOGOROV-JOHNSON-MEHL-AVRAMI THEORY

Let us consider an amorphous matrix of volume V_{cell} containing N isolated grains of volumes ν_i, $i=1,\ldots,N$. Let $V(t)$ be the volume of the crystalline part of the system (crystalline volume). Until the grains are separated $V(t)=\Sigma_{i=1,N}\nu_i$. At variance, when the grains are so large to touch each other, it is useful to introduce the crystalline extended volume $V_{\text{ext}}(t)$ which is defined as the total volume that the same N crystalline grains would occupy if they were isolated and they could grow through each other without mutual interference. It is useful to normalize $V(t)$ and $V_{\text{ext}}(t)$ with respect to the total volume V_{cell}, so obtaining the crystallinity $\chi(t)$ and the extended crystallinity $\chi_{\text{ext}}(t)$, respectively. It turns out that $\chi_{\text{ext}}(t) \geq \chi(t)$ since, by definition, the extended crystallinity double counts the overlap regions. In particular, within the PLG model it is found that the extended volume increases arbitrarily with time [$\chi_{\text{ext}}(t) \to \infty$ as $t \to \infty$], while $\chi(t)$ is always smaller than the unity.

Under the assumptions of isotropic growth and spatially random nucleation[21] (see Sec. I), the KJMA formula,[15]

$$\chi(t) = 1 - e^{\chi_{\text{ext}}(t)}, \tag{19}$$

provides the crystalline fraction as a function of the normalized extended volume. Equation (19) is extensively used since it makes it possible to bypass the difficult calculation of the overlap volumes. In order to calculate $\chi(t)$, it is therefore necessary to calculate $\chi_{\text{ext}}(t)$ that, in turn, is easily obtained by $J(t)$ and $\nu(t)$ through the relation

$$V_{\text{ext}}(t) = \int_0^t \nu(\tau) J(t-\tau) d\tau. \tag{20}$$

At time $t=0$ the system is supposed to be completely amorphous [i.e., $V_{\text{ext}}(t)=0$]. In this work we calculate Eq. (19) under the assumption of site-saturated crystallization. We further assume that rate of nucleation J_0 is a constant during the nucleation period (i.e., $J_0=N/t_N$). We get

$$J(t) = J_0[h(t) - h(t-t_N)], \tag{21}$$

where $h(t)$ is the Heavside step function. By inserting Eq. (21) into Eq. (20) the following equation is obtained:

$$V_{\text{ext}} = J_0 \frac{\beta}{p+1}[t^{p+1} - (t-t_N)^{p+1} h(t-t_N)]. \tag{22}$$

It is possible to distinguish two cases, hereafter named synchronous site-saturated crystallization (SSSC) and asynchronous site-saturated crystallization (ASSC). The SSSC occurs when t_N is vanishingly small (i.e., when $t_N/t \to 0$) and $J(t) \sim N\delta(t)$. The grains nucleate at $t=0$ and their growth is synchronous since each grain will have the same volume $\nu(t)$ at any later time $t>0$. The corresponding SSSC extended crystalline fraction is

$$V_{\text{ext}}(t) = N\beta t^p. \tag{23}$$

On the other hand, ASSC is observed when (after the nucleation time) the grains do not have the same size. This occurs when $t_N/t \sim 1$. Under these conditions, Eq. (22) becomes

$$V_{\text{ext}} = J_0 \frac{\beta}{p+1}[t^{p+1} - (t-t_N)^{p+1}]. \tag{24}$$

During the ASSC the extended volume of each grain lies within the range $[\nu(t-t_N), \nu(t)]$. Within the PLG model this range depends on time $[\beta(t-t_N)^p, \beta t^p]$. Similarly, the radii of the grains $R_i \sim \nu_i^{1/2}$ are not identical and lies within a range

$$[R_{\min}, R_{\max}] = [R_{\min}, R_{\min} + \Delta R], \tag{25}$$

where $\Delta R(t) = \max_{i \neq j} |R^i(t) - R^j(t)|$. It is easy to prove that when $t > t_N$,

$$0 < \Delta R(t) = \alpha(t^q - (t-t_N)^q) < \alpha t_N^q. \tag{26}$$

We remark that $\Delta R(t)$ increases with the nucleation time t_N. Equation (26) is valid also in the limit of SSSC, i.e., when $t_N/t \to 0$. In this case, $\Delta R \to 0$ since all the grains have the same dimension.

It is important to note that the KJMA equation makes it possible to estimate the growth exponent p (or q). In the SSSC, the exponent p is obtained by combining Eqs. (19) and (24),

$$p = \frac{1}{\ln t} \ln\{-\ln[1 - \chi(t)]\}. \tag{27}$$

We remark that in the case of asynchronous growth, Eq. (27) is no longer valid since it is necessary to use Eq. (24) instead of Eq. (23) in order to fit the crystallinity. The parameters p, t_N, and α (or β) are outcomes of the fitting procedure.

Present atomistic simulations correspond to the ASSC since no grain nucleation was observed and $\Delta R > 0$. It is important to stress that our model of crystallization includes realistic features indeed present in real experiments; moreover, such features are beyond the conditions of validity of the KJMA theory for at least three reasons: (i) first of all, it takes into account the anisotropic growth of grains[7] and the fact that the grains are randomly oriented; (ii) second, there are size effects (e.g., the number of grains is finite and their radii are comparable with the overall volume); and (iii) the

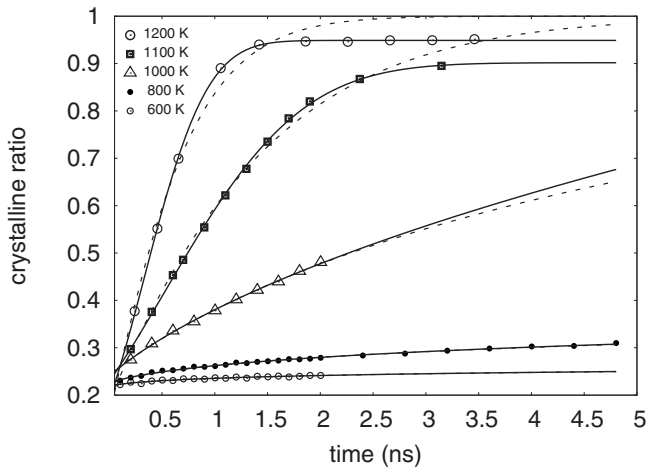

FIG. 5. Crystallinity $\chi(t)$ as a function of the annealing time after nucleation. Dashed and continuous lines are fits based on the KJMA theory and KJMA-N renormalized theory, respectively.

grain growth is affected by the presence of neighboring grains and by their relative crystallographic orientation. Accordingly, we expect in principle that KJMA cannot fully reproduce the atomistic data. However, we are going to demonstrate that KJMA is nevertheless able to provide an overall picture which is not that different from the atomistic one. To this aim the crystalline fraction $\chi(t)$ of each system was calculated during a constant-temperature annealing as a function of the annealing time. The atomistic data were fit by inserting Eq. (24) for the asynchronous growth into Eq. (19) and by using t_N, α, and the exponent p as adjustable parameters. The results are represented as dashed curves in Fig. 5 and show that the fit works well at small crystallization times. Furthermore, the actual nucleation time t_N can be estimated by using the grain-size distribution ΔR and our growth model [Eq. (16)]; it is easily obtained $t_N \sim (\Delta R)^{1/q}$. We found t_N of the order of 1.0 ns.

From the same analysis, we calculated the exponent $q=p/2$ and α of Eq. (24). Both quantities are predicted to be independent of the number N. Actually, as reported in Fig. 2, the exponents calculated from the distribution of grains turn out to be quite close to the case of the isolated grain. Since the exponents control the asymptotic time evolution of the grains, we conclude that the interaction of the grains affects the growth exponents although not dramatically.

Concerning the prefactor α, Fig. 6 shows that it is slightly smaller in the case of a distribution of grains at temperatures $T<T_{ma}$. We attribute such a difference to the interference between the neighboring grains that makes the growth less efficient.

The most important deviation from the KJMA theory concerns the asymptotic crystalline ratio. The atomistic values of crystallinity are, in fact, always smaller than predicted by KJMA and we found $\chi=0.90$, 0.95, and 0.99 at 1100, 1200, and 1400 K, respectively. At temperatures $T<1100$ K, the crystallization is so slow that the average crystallinity is always below 0.35 at any simulated time. Accordingly, it is difficult to calculate accurately the asymptotic crystallinity at such lower temperatures. The incomplete crystallization observed at high temperature is due to the formation of defects

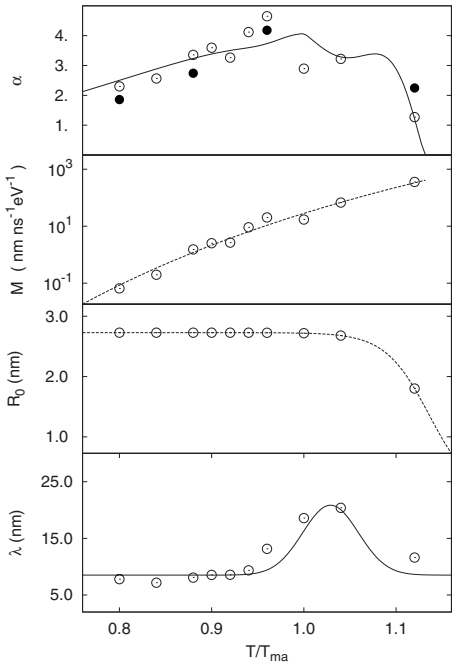

FIG. 6. Temperature dependence of growth parameters: λ, R_0, M, and α. Continuous lines are analytical models; open symbols are calculated from the growth of the isolated grain; filled symbols (top panel) are obtained by fitting the KJMA model in the case of a distribution of grains.

in the final microstructure. As shown in Fig. 1 (bottom panel), the final microstructure contains both grain boundaries and spotlike amorphous regions. Both defects depend on the temperature and prevent the formation of a perfect crystalline structure. We also observe that, as the temperature increases, the system is able to reach a higher degree of crystallinity. It is important to note that such a saturation depends on atomic-scale details of the microstructure and it cannot be predicted within the KJMA theory. We finally note that such effects are not related to the finite size the system, rather on the actual microstructure of the boundaries.

In order to improve the agreement of KJMA theory with the atomistic data it is necessary to renormalize the KJMA function. This approach will be hereafter referred to as KJMA-N phenomenological equation. The idea is to normalize both the crystallized volume and the extended one by the same asymptotic crystalline ratio χ_∞. Such a quantity is unknown *a priori*, but it is used as a disposable parameter to be fit on of the atomistic data. The results are reported in Fig. 5. The KJMA-N phenomenological equation describes accurately the atomistic data for any crystallinity, providing different exponents than standard KJMA theory (see Fig. 2). This proves that the exponents calculated from KJMA-N are not the growth exponents of the isolated grain, unless we limit the fit to the initial annealing time when the grains are isolated. By using the KJMA-N for a global fit it is found an overall agreement at all the temperatures considered, but a small overestimation of the exponents.

V. CONCLUSIONS

In conclusion, we have studied the growth of both an isolated and a distribution of cylindrical grains embedded

into an amorphous Si matrix. We proved that the growth of an isolated grain can be described by a power-law model and we have fully characterized the dependence of the radius evolution both on time and temperature. Furthermore, we studied the case of a distribution of grains and we have focused on the case of site-saturated crystallization. By comparing the results with the case of an isolated grain, we found that the KJMA theory is unable to reproduce accurately the crystallinity dependence upon time. Such deviations are due to the fact that the atomistic model of crystallization includes features that are out of reach of the KJMA theory (as, for example, anisotropic grain growth or finite-size effects). In order to reconcile the atomistic results with the continuum KJMA theory, we use an improved KJMA-N function where the asymptotic crystallinity is normalized to the actual value obtained from atomistic simulations. Finally, the atomistic data prove that the asymptotic crystallinity increases with the annealing temperature.

ACKNOWLEDGMENTS

This work has been funded by EU under project EU-STREP NanoPhoto and by MIUR under Project PON-Cybersar. We acknowledge computational and technical support by CASPUR Rome.

APPENDIX

In order to find the T dependence of $R(t,T)$ [Eq. (16)], we need to estimate the functions $g_{ac}(T)$, $M(T)$, $\lambda(T)$, and $R_0(T)$. The T dependence of $q(T)$ is reproduced by the fitting curve

$$q(T) = q_1 + q_2\left\{\frac{1}{2} + \frac{1}{\pi}\arctan\left[q_3\left(\frac{T}{T^*} - 1\right)\right]\right\}, \quad \text{(A1)}$$

where $q_1=0.0841$, $q_2=1.49$, $q_3=16.34$, and $T^* \simeq T_{ma}$ were adjusted to reproduce the atomistic data. The model corresponds to the curve of Fig. 2 and it was chosen as a prototype of a smooth step function.

As far as the free energy $g_{ac}(T)$, we used the experimental data of Grimaldi *et al.*[31] In order to compare experiments and simulations, we rescaled all the temperatures by the amorphous melting temperature T_{ma}. Such a procedure is legitimate since the ratio $T_{mc}/T_{ma}=1.16$ is very accurately reproduced by the EDIP potential. At variance, it is found that the EDIP value for T_{ma} (T_{mc}) is 1250 K (1450 K), smaller than the experimental value 1470 K (1693 K). At temperatures in the range $T<T_{ma}$ the free energy was found to decrease (approximately) linearly with the temperature. At $T_0=600$ K it is found $g_{ac}(T_0)=g^0 \sim 0.11$ eV/atom while $g_{ac}(T_{ma})=g^{ma} \sim 0.09$ eV/atom at T_{ma}. Accordingly we get

$$g_{ac}(T) = g_0 + \frac{g_{ma} - g_0}{T_{ma} - T^0}(T_{ma} - T) \quad T_0 < T < T_{ma}. \quad \text{(A2)}$$

At temperatures $T>T_{ma}$, the liquid phase is thermodynamically more stable than the amorphous phase. Accordingly, the free-energy curve g_{ac} to be considered in Eq. (16) is the difference between the liquid and the crystal phase. Also in this case the dependence on the temperature is linear and it may be modeled by

$$g_{ac}(T) = g_{ma} - \frac{g_{ma}}{T_{mc} - T_{ma}}(T_{ma} - T) \quad T_{ma} < T < T_{mc}. \quad \text{(A3)}$$

Equations (A2) and (A3) give the overall temperature dependence of $g_{ac}(T)$.

The boundary mobility $M(T)$ is computed by assuming a single activation energy E_a, i.e.,

$$M(T) = \mu e^{-E_a/k_B T}/k_B T. \quad \text{(A4)}$$

It is possible to fit our data with an activation energy $E_a \sim 2.6$ eV close to the experimental value 2.7 eV.[29] The prefactor μ was found to be $\sim 1.8\times 10^9$ nm^3 ns^{-1}. The calculated mobility and the analytical fit are reported in Fig. 6 as a function of the temperature. We observe that the calculated boundary mobility $M(T)$ is a few orders of magnitude larger than the experimental data.[32] This discrepancy is not a consequence of the method used to calculate M in the present analysis. Rather, such an overestimation is found also when studying the crystallization of a planar interface[25] [solid phase epitaxy (SPE)] and it is a common feature of the available model potentials for SPE in silicon.[32] The choice of the EDIP potential is legitimate and favorable because it makes a fast crystallization affordable.

The quantity R_0 appearing in Eq. (16) is the initial grain radius for an annealing at a fixed temperature. As explained in Sec. II, R_0 depends on the annealing temperature T. In the range 1000 K$<T<$1400 K the function $R_0(T)$ is

$$R_0(T) = \frac{R_1}{1 + e^{R_3(R_2 - T)}}, \quad \text{(A5)}$$

where $R_1=2.728$ nm, $R_2=1419$ K, and $R_3=0.034$ K^{-1} (see Fig. 6).

Finally, let us consider the temperature dependence of $\lambda(T)$ which is the length scale controlling the nonuniform growth of Eq. (16). Such a quantity is related to the faceting of the grain. For a given temperature and a given growth exponent, a larger λ gives a larger velocity and a stronger nonuniform character of the growth. $\lambda(T)$ is a nonmonotonic function of the temperature in the range $1000<T<1400$ K where it is found 8 nm$<\lambda<$25 nm (see Fig. 6). We found

$$\lambda(T) = \lambda_0 + \lambda_1 e^{-(T/\delta - \tau)^2} \quad \text{(A6)}$$

where $\lambda_0=8.515$ nm, $\lambda_1=12.36$ nm, $\delta=53.28$ K, and $\tau=24.14$. $\lambda(T)$ is found to have a peak close to the amorphous melting temperature T_{ma} where $q \to 1$. This reminds a divergence at the transition temperature (see Fig. 6).

The set of functions $\{q(T), M(T), g_{ac}(T), \lambda(T)\}$ described above gives the temperature dependence of the frequency $\Gamma(T)$ appearing in Eq. (16). We found 8×10^{-3} ns$^{-1}<\Gamma<0.5$ ns^{-1}. By combining $\Gamma(T)$ and $R_0(T)$ the dependence on time and temperature of the grain radius is given and it is able to model the whole set of calculated atomistic data.

*alessandro.mattoni@dsf.unica.it
†luciano.colombo@dsf.unica.it

[1] C. Spinella, S. Lombardo, and F. Priolo, J. Appl. Phys. **84**, 5383 (1998).
[2] F. Cleri and P. Keblinski, Int. J. Comput. Eng. Sci. **2**, 242 (2006).
[3] S. Pizzini, M. Acciarri, S. Binetti, D. Cavalcoli, A. Cavallini, D. Chrastina, L. Colombo, E. Grilli, G. Isella, M. Lancin, A. Le Donne, A. Mattoni, K. Peter, B. Pichaud, E. Poliani, M. Rossi, S. Sanguinetti, M. Texier, and H. Von Känel, Mater. Sci. Eng., B **134**, 118 (2006).
[4] J. D. Kuntz, G. Zhan, and A. K. Mukherjee, MRS Bull. **29**, 22 (2004).
[5] H. Awaji, S.-M. Choi, and E. Yagi, Mech. Mater. **34**, 411 (2002).
[6] N. Sakudo, N. Ikenaga, H. Yasui, and K. Awazu, Proceedings of the Sixth International Conference on Coatings on Glass and Plastic (ICCG6), 2006 (unpublished), p. 79.
[7] A. Mattoni and L. Colombo, Phys. Rev. Lett. **99**, 205501 (2007).
[8] R. B. Iverson and R. Reif, J. Appl. Phys. **62**, 1675 (1987).
[9] G. Shi and H. Seinfeld, J. Mater. Res. **6**, 2091 (1991).
[10] G. Shi and H. Seinfeld, J. Mater. Res. **6**, 2097 (1991).
[11] W. A. Johnson and R. F. Mehl, Trans. Am. Inst. Min., Metall. Pet. Eng. **135**, 416 (1939).
[12] M. Avrami, J. Chem. Phys. **7**, 1103 (1939).
[13] M. Avrami, J. Chem. Phys. **8**, 212 (1940).
[14] A. N. Kolmogoroff, Bull. Acad. Sci USSR. Ser. Math. **3**, 355 (1937).
[15] M. Fanfoni and M. Tomellini, Phys. Rev. B **54**, 9828 (1996).
[16] J. W. Christian, *The Theory of Phase Transformations in Metals and Alloys* (Pergamon, Oxford, 1975), Pt. I.
[17] M. Castro, F. Domìnguez-Adame, A. Sànchez, and T. Rodrìguez, Appl. Phys. Lett. **75**, 2205 (1999).
[18] A. A. Burbelko, E. Fraś, and W. Kapturkiewicz, Mater. Sci. Eng., A **413-414**, 429 (2005).
[19] B. A. Berg and S. Dubey, Phys. Rev. Lett. **100**, 165702 (2008).
[20] M. Castro, A. Sanchez, and F. Dominguez-Adame, Phys. Rev. B **61**, 6579 (2000).
[21] J. Farjas and P. Roura, Phys. Rev. B **75**, 184112 (2007).
[22] E. Pineda, T. Pradell, and D. Crespo, Philos. Mag. A **82**, 107 (2002).
[23] P. Bruna, D. Crespo, and R. González-Cinca, J. Appl. Phys. **100**, 054907 (2006).
[24] J. F. Justo, M. Z. Bazant, E. Kaxiras, V. V. Bulatov, and S. Yip, Phys. Rev. B **58**, 2539 (1998).
[25] N. Bernstein, M. J. Aziz, and E. Kaxiras, Phys. Rev. B **61**, 6696 (2000).
[26] A. Mattoni and L. Colombo, Europhys. Lett. **62**, 862 (2003).
[27] A. Mattoni and L. Colombo, Phys. Rev. B **69**, 045204 (2004).
[28] D. S. Franzblau, Phys. Rev. B **44**, 4925 (1991).
[29] G. L. Olson and J. A. Roth, Mater. Sci. Rep. **3**, 1 (1988).
[30] M. O. Thomson, G. J. Galvin, J. W. Mayer, P. S. Peercy, J. M. Poate, D. C. Jacobson, A. G. Cullis, and N. G. Chew, Phys. Rev. Lett. **52**, 2360 (1984).
[31] M. G. Grimaldi, P. Baeri, and M. A. Malvezzi, Phys. Rev. B **44**, 1546 (1991).
[32] C. Krzeminski, Q. Brulin, V. Cuny, E. Lecat, E. Lampin, and F. Cleri, J. Appl. Phys. **101**, 123506 (2007).